Molecular Biology of the Cell
Vol. 10, 1939–1955, June 1999

Localization and Recycling of gp27 (hp24γ_3): Complex Formation with Other p24 Family Members

Joachim Füllekrug,* Tatsuo Suganuma,† Bor Luen Tang,‡ Wanjing Hong,‡ Brian Storrie,§ and Tommy Nilsson*‖

*Cell Biology and Cell Biophysics Program, European Molecular Biology Laboratory, 69117 Heidelberg, Germany; †Department of Anatomy, Miyazaki Medical College, Miyazaki 889-1692, Japan; ‡Membrane Biology Laboratory, Institute of Molecular and Cell Biology, Singapore 117609, Republic of Singapore; and §Department of Biochemistry, Virginia Polytechnic Institute and State University, Blacksburg, Virginia 24061-0308

Submitted October 19, 1998; Accepted March 17, 1999
Monitoring Editor: Chris Kaiser

We report here the characterization of gp27 (hp24γ_3), a glycoprotein of the p24 family of small and abundant transmembrane proteins of the secretory pathway. Immunoelectron and confocal scanning microscopy show that at steady state, gp27 localizes to the *cis* side of the Golgi apparatus. In addition, some gp27 was detected in COPI- and COPII-coated structures throughout the cytoplasm. This indicated cycling that was confirmed in three ways. First, 15°C temperature treatment resulted in accumulation of gp27 in pre-Golgi structures colocalizing with anterograde cargo. Second, treatment with brefeldin A caused gp27 to relocate into peripheral structures positive for both KDEL receptor and COPII. Third, microinjection of a dominant negative mutant of Sar1p trapped gp27 in the endoplasmic reticulum (ER) by blocking ER export. Together, this shows that gp27 cycles extensively in the early secretory pathway. Immunoprecipitation and coexpression studies further revealed that a significant fraction of gp27 existed in a hetero-oligomeric complex. Three members of the p24 family, GMP25 (hp24α_2), p24 (hp24β_1), and p23 (hp24δ_1), coprecipitated in what appeared to be stochiometric amounts. This heterocomplex was specific. Immunoprecipitation of p26 (hp24γ_4) failed to coprecipitate GMP25, p24, or p23. Also, very little p26 was found coprecipitating with gp27. A functional requirement for complex formation was suggested at the level of ER export. Transiently expressed gp27 failed to leave the ER unless other p24 family proteins were coexpressed. Comparison of attached oligosaccharides showed that gp27 and GMP25 recycled differentially. Only a very minor portion of GMP25 displayed complex oligosaccharides. In contrast, all of gp27 showed modifications by medial and *trans* enzymes at steady state. We conclude from these data that a portion of gp27 exists as hetero-oligomeric complexes with GMP25, p24, and p23 and that these complexes are in dynamic equilibrium with individual p24 proteins to allow for differential recycling and distributions.

INTRODUCTION

Transport through the secretory pathway is initiated through concentration of newly synthesized proteins into COPII-coated buds. These pinch off the endoplasmic reticulum (ER) and accumulate as clusters at the peripheral ER exit sites (Aridor *et al.*, 1995). The clusters, termed the ER-to-Golgi intermediate compartment (ERGIC) or pre-Golgi transport intermediates, next recruit COPI and move toward the central juxtanuclear Golgi apparatus along microtubules (Saraste and Svensson, 1991; Presley *et al.*, 1997; Scales *et al.*, 1997). At the Golgi apparatus, anterograde cargo is then delivered for further transport. In the recent past, genetic and biochemical studies have identified and

‖ Corresponding author. E-mail address: nilsson@embl-heidelberg.de.

characterized a variety of proteins required for intracellular transport. These include coat proteins, small GTPases (e.g., rabs, arf, and sar1p), *N*-ethyl maleimide-sensitive factor (NSF), soluble NSF attachment proteins, and soluble NSF attachment protein receptor proteins, all of which play key roles in transport (reviewed by Rothman, 1994).

Apart from soluble NSF attachment protein receptor proteins, most if not all identified components of the transport machinery were of cytoplasmic origin. Recently, a family of small and abundant type I integral membrane proteins, termed p24, was discovered (Wada *et al.*, 1991; Schimmöller *et al.*, 1995; Stamnes *et al.*, 1995; Belden and Barlowe, 1996; Blum *et al.*, 1996; Sohn *et al.*, 1996; Gayle *et al.*, 1996; Rojo *et al.*, 1997; Dominguez *et al.*, 1998). This family is of unknown function, although at least some evidence argues that they play important roles in transport (Schimmöller *et al.*, 1995; Belden and Barlowe, 1996; Rojo *et al.*, 1997). Their overall homology is ~30% at the amino acid level. Because some p24 proteins show higher degree of homology to each other than do others, this results in an apparent subfamily division (Dominguez *et al.*, 1998). Based on this and order of discovery, we proposed a nomenclature building on previous ones to allow for an accurate comparison between species. A p24 protein is according to this nomenclature preceded by one letter to define the species (e.g., h for human) followed by p24, the subfamily (α, β, δ, or γ) and a number, which indicates order of discovery (e.g., hp24α_2). This division into α, β, δ, and γ implies that they are part of a larger complex, and data presented in this study show that they are.

The notion that p24 proteins play important roles in transport stems from several lines of evidence. Deletion of two of the eight p24 proteins in yeast, emp24p (yp24β_1) and erv25p (yp24δ_1), caused a decrease in anterograde transport of some cargo. This and their observed abundance in COPII vesicles led to the suggestion that p24 proteins mediate active cargo selection in the ER (Schimmöller *et al.*, 1995; Belden and Barlowe, 1996). Also, deletion of emp24 resulted in secretion of the ER-resident Kar2p, suggesting a role in maintaining a functional ER retention and retrieval machinery (Elrod-Erickson and Kaiser, 1996). In mammalian cells, p24 proteins were suggested to serve as the primary receptors for COPI and, hence, to be essential components in forward vesicular transport (Stamnes *et al.*, 1995; Sohn *et al.*, 1996). p23 (hp24δ_1) and p24 (hp24β_1) were identified as major constituents of COPI-coated Golgi-derived vesicles. Also, p23 was suggested to play a structural role in the *cis*-Golgi network (CGN), and microinjection of antibodies directed toward its cytoplasmic domain blocked transport of newly synthesized proteins, suggesting a role in anterograde transport (Rojo *et al.*, 1997). However, the observation that p24 proteins reside at steady state in the early part of the secretory pathway makes it unlikely that p24 proteins play a role in forward transport beyond the *cis*-Golgi (Rojo *et al.*, 1997; Dominguez *et al.*, 1998).

Strong data exist showing that p24 proteins bind cytoplasmic coat proteins. The first p24 protein to be identified, gp25l (hp24α_1), was isolated as an abundant calnexin-binding protein of the ER (Wada *et al.*, 1991). This protein displays in its cytoplasmic domain three discrete motifs. The first, FF, is conserved throughout the p24 family and is, in some members, part of a larger motif, F/YXXXXF/Y. The FF motif has been shown to be required for transport out of the ER and mediates a direct interaction with coat components of COPII complex (Dominguez *et al.*, 1998). The second motif, K(X)KXX, situated closer to the C terminus, is also conserved among the p24 proteins but to a lesser extent. Whereas all p24α proteins display a typical K(X)KXX motif, the other members show variations of this motif. For example, p23 (hp24δ_1) and p24 (hp24β_1) have one additional amino acid or two lysines substituted to arginines, respectively, rendering these less efficient in COPI binding (Dominguez *et al.*, 1998). A third motif, situated at the extreme C terminus of p24α, β, and δ proteins, shows similarities with the $\phi\phi$ motif involved in endocytic sorting. The role of the $\phi\phi$ motif in p24 proteins is less clear, although a recent study suggests that they enhance exit rates out of the ER (Nakamura *et al.*, 1998). Taken together, this abundant and well-conserved family of membrane proteins are likely to play a role in trafficking between the ER and the Golgi apparatus. To further characterize this role, we have undertaken a detailed study of hp24γ_3 (gp27) and show that it resides in the *cis*-Golgi from where it recycles to earlier compartments, including the ER. We find that gp27 is part of a heterotypic complex with three other p24 proteins, GMP25, p24, and p23, and that such complex formation is required for exit out of the ER. By analyzing the N-linked oligosaccharide composition of gp27, we also show that although p27 participates in heterotypic complex formation, its oligosaccharide is readily converted into complex structures. Under the same conditions, the N-linked oligosaccharide of GMP25 is not converted, suggesting that p24 proteins exist in a dynamic equilibrium between complexed and single proteins.

MATERIALS AND METHODS

Antibodies

Antibodies against gp27 and p26 were raised in rabbits according to standard procedures using peptides corresponding to amino acids 196–211 of human gp27 (KSFFSDKRTTTTRVGS) and amino acids 202–217 of human p26 (KSFFTEKRPISRAVHS) coupled to keyhole limpet hemocyanin. Affinity purification of antiserum using a peptide-agarose column was as recommended by the manufacturer (Pierce, Rockford, IL). An aliquot of affinity-purified antibodies was

biotinylated with sulfosuccinimidyl-6-(biotinamido)-hexanoate. Antibodies against other p24 family proteins (p23, p24, GMP25, and gp27/p26) have been described (Dominguez *et al.*, 1998). The following mAbs were concentrated from hybridoma supernatant: myc (9E10; Evan *et al.*, 1985), VSV-G (P5D4; Kreis, 1986) and β′-COP (CM1A10; Palmer *et al.*, 1993). Monoclonal purified mouse antibodies against β1,4-galactosyltransferase (GalT [GTL2]; Kawano *et al.*, 1994) and affinity-purified rabbit antibodies directed against Sec13 (Tang *et al.*, 1997) were used for immunofluorescence. A polyclonal rabbit antiserum (N10) against GalT (Eric G. Berger, Institute for Physiology, Zürich, Switzerland; Watzele *et al.*, 1991) and rabbit antisera against KDEL receptor and p23 (H.D. Söling, Max-Planck-Institut for Biophysical Chemistry, Göttingen, Germany) were kindly provided. Caveolin antibodies (N20) were from Santa Cruz Biotechnology (Santa Cruz, CA). Mouse anti-biotin monoclonal antiserum was from Boehringer Mannheim (Mannheim, Germany). Rabbit immunoglobulin G (IgG) used for blocking in the double-labeling protocol was from Sigma (St. Louis, MO). The following secondary antibodies were used: donkey anti-rabbit coupled to Cy3 or FITC and donkey anti-mouse FITC or Cy3 (Dianova, Hamburg, Germany).

Cell Culture and Viral Infection

HeLa, Vero, and hybridoma (CM1A10 and P5D4) cells were grown in Dulbecco's minimal essential medium (DMEM) supplemented with 10% FBS under standard tissue culture conditions. NI-Vero cells stably transfected with myc-tagged *N*-acetylglucosaminyltransferase I (NAGT I; Yang and Storrie, 1998) were maintained in the presence 0.2 mg/ml G-418.

Vesicular Stomatitis Virus strain tsO45 (kindly provided by Kai Simons, European Molecular Biology Laboratory [EMBL]) was used to infect Vero cells for 45 min at room temperature in DMEM and 20 mM HEPES, pH 7.2, without FBS. Accumulation of VSV glycoprotein G (VSV-G^{ts045}) was for 3 h at 39.5°C in DMEM including FBS. Subsequent incubation at 15°C was in the presence of 200 μM cycloheximide.

gp27 Expression Plasmid and DNA Transfection

Expression plasmids for the different p24 family proteins have been described previously (Dominguez *et al.*, 1998). To enable more efficient expression and visualization of transfected gp27, an epitope-tagged form of gp27 cDNA was constructed. The final cDNA, inserted into pcDNA3 (Invitrogen, Carlsbad, CA), encodes a gp27/VSV-G having a signal sequence of the human CD8 followed by the VSV-G epitope (recognized by the mAb P5D4) followed by the mature gp27 protein. The epitope tag did not lead to retention or misfolding in the ER, because a chimeric protein with the transmembrane domain and cytoplasmic tail of the plasma membrane protein CD8 was transported efficiently through the secretory pathway and was expressed at the cell surface (our unpublished results).

Transfections were carried out according to the calcium phosphate coprecipitation method (Keown *et al.*, 1990). Three micrograms of plasmid DNA were applied for transfection of subconfluent HeLa cells (10 cm^2). For coexpression experiments, 0.6 μg of each single plasmid were used, and the remaining amount of DNA was made up with pcDNA3. Cells were processed for immunofluorescence 24 h after transfection. Brefeldin A (Epicentre Technologies, Madison, WI) was used at a concentration of 5 μg/ml for 30 min at 37°C.

Immunofluorescence Confocal Analysis and Microinjection

Cells grown on coverslips were fixed with 3% paraformaldehyde for 20 min. After quenching aldehyde groups with ammonium chloride, cells were permeabilized with 0.1% saponin. Antibodies were incubated in PBS containing 0.2% fish skin gelatin and 0.1% saponin. Double immunofluorescence labeling with two rabbit antibodies was done sequentially: Sec13 or KDEL receptor antiserum, donkey anti-rabbit FITC (6 μg/ml), rabbit IgG (40 μg/ml), gp27-biotin, mouse anti-biotin, and donkey anti-mouse Cy3 (1.5 μg/ml). No cross-reaction was observed in control experiments. Coverslips were mounted in Moviol and viewed with a Zeiss (Thornwood, NY) Axiovert 100TV microscope equipped with a 24-bit red–green–blue three-chip charge-coupled device (Hamamatsu Photonics, Hamamatsu City, Japan; Improvision, Coventry, United Kingdom) or a Leica (Wetzlar, Germany) confocal microscope.

Confocal images were acquired in the following way. Laser intensity was adjusted to give maximum signal without any bleed-through into the respective other channel. Before final scanning, both channels were checked in "glow over" mode to ensure that the maximum fluorescence intensity was still in the recording range. Images were obtained simultaneously to exclude any artifacts from sequential acquisition. Only one focal plane was analyzed. Staining shifted against each other was confirmed by series of z sections and repeated simultaneous scans. Micrographs were arranged with Adobe Photoshop and Illustrator (Adobe Systems, Mountain View, CA).

Expression plasmid encoding for the mutant Sar1 protein ($Sar1p^{dn}$) was a kind gift from Dr. W.E. Balch (Scripps Clinic and Research Foundation, La Jolla, CA) and was used to produce recombinant protein according to standard procedures (Rowe and Balch, 1995). $Sar1p^{dn}$ was mixed with Cascade blue BSA (Molecular Probes, Eugene, OR) as a coinjection marker to give a final concentration of 1.5 mg/ml $Sar1p^{dn}$. The protein was injected into HeLa or Vero cells with an Eppendorf (Hamburg, Germany) microinjection system in the presence of 5 μg/ml emetine to inhibit protein synthesis. Cells were incubated after injection in the continuous presence of emetine.

Electron Microscopy

Immunogold labeling and electron microscopy of thawed cryosections were performed as described previously (Griffiths, 1993). Briefly, HeLa cells were fixed for 3 h at room temperature. with 0.2% glutaraldehyde and 2% paraformaldehyde in PBS. Cell pellets were embedded in 10% gelatin, trimmed, infiltrated with 2.1 M sucrose, and frozen in liquid nitrogen. Ultrathin sections were cut at −100°C, picked up in 2.3 M sucrose, and transferred to Formvar- and carbon-coated copper grids. Double labeling was done sequentially using different sizes of protein A-colloidal gold. After labeling procedures, 0.3% uranyl acetate in 2% methyl cellulose was used for staining and embedding. Sections were viewed with a Zeiss EM10 microscope, and pictures were taken at magnifications of 32,000 or 65,000×.

Immunoprecipitation and Two-dimensional Gel Electrophoresis

In pilot experiments, solubilization of gp27 was investigated. HeLa cells were harvested in PBS on ice and sedimented for 5 min at 500 × *g*. The cell pellet (corresponding to an area of 7.5 cm^2 of the Petri dish) was treated with 200 μl of 1% (vol/vol) Triton X-100 (TX-100) in lysis buffer (50 mM Tris, pH 7.4, 100 mM NaCl, and 2 mM EDTA) for 15 min on ice. The solution was centrifuged for 10 min at 20,000 × *g*. Proteins from supernatant and pellet were precipitated with trichloroacetic acid, washed with methanol, neutralized by addition of 1 M Tris, pH 9.0, and analyzed by SDS-PAGE and Western blotting. A control sample was lysed with SDS-PAGE loading buffer. Solubilization of gp27 was efficient (see Figure 7a, inset).

For immunoprecipitation, HeLa cells were labeled overnight with 0.25 mCi of [^{35}S]methionine/ml of medium. Lysis was done on ice for 15 min in the presence of 1% (vol/vol) TX-100 or 0.4% SDS in lysis buffer. SDS samples were sonicated to shear chromosomal DNA, and TX-100 was added to quench SDS. After centrifugation

and preclearing with 20 μl of protein A-Sepharose/ml lysate, antibodies were added and incubated for 60 min at room temperature. Immunoprecipitates were collected with 20 μl of protein A-Sepharose for 30 min at room temperature. The pellet was washed three times with lysis buffer containing 0.1% TX-100 (0.5% TX-100 and 0.1% SDS for the samples lysed with SDS), two times with 0.5 M NaCl and 0.05% TX-100, and two times with 50 mM Tris, pH 7.4. Pellets were dissolved in SDS sample buffer or isoelectric focusing lysis buffer (1% [vol/vol] NP-40 and 8 M urea). Unlabeled Golgi-enriched membrane fraction was prepared from HeLa cells as described by Dominguez *et al.* (1998). Thirty micrograms of protein of fraction 4 were mixed with immunoprecipitate for the two-dimensional (2D) gel shown in Figure 7, a and b. 2D gel electrophoresis was done in a Bio-Rad (Hercules, CA) Mini-Protean II 2D cell according to the manufacturer's recommendations, except for the composition of isoelectric focusing tube gels (2.87 g of urea, 670 μl of acrylamide mix, 1.01 ml of 10% NP-40, 139 μl of ampholines 5–7 [Serva, Heidelberg, Germany], 139 μl of ampholines 5–7 [Pharmacia, Uppsala, Sweden], 101 μl of ampholines 3.5–10 [Pharmacia], 8 μl of *N,N,N′,N′*-tetramethylethylenediamine, and 8 μl of 10% ammonium peroxodisulfate. Gels were transferred to nitrocellulose and either exposed to x-ray film or processed for Western blotting using HRP coupled to protein A. 2D gels separating immunoprecipitates without unlabeled Golgi fraction showed less horizontal streaking than shown in Figure 7, a and b, and were quantified with a PhosphorImager (Molecular Dynamics, Sunnyvale, CA).

Deglycosylation and Pulse–Chase Analysis

Golgi-enriched subcellular fractions from HeLa cells (20 μg of protein) or rat liver Golgi membranes (10 μg) were treated with or without 1 U of peptide-*N*-glycosidase F, 10 mU of endoglycosidase H (Endo H), or 50 mU of neuraminidase (*Vibrio cholerae*) according to the recommendations of the supplier (Boehringer Mannheim). Proteins were separated by 14% SDS-PAGE and analyzed by Western blotting.

HeLa cells were depleted of endogenous methionine by incubating for 15 min at 37°C in methionine-free labeling medium, pulsed with 100 μCi of [^{35}S]methionine/10 cm^2 (0.25 mCi/ml specific activity) for 15 min, and chased with an excess of unlabeled methionine for 0, 15, 60, and 240 min. Lysis was on ice for 15 min in the presence of 1% (vol/vol) TX-100. Immunoprecipitation was as described (see above), except that the initial immunoprecipitate was washed five times with 0.1% SDS and 0.5% TX-100 and subsequently treated with 3 mU of Endo H overnight.

RESULTS

Localization of gp27 to the CGN and cis-Cisterna of the Golgi Apparatus

We previously reported the cloning and preliminary characterization of gp27 (hp24γ_3), a member of the p24 family of transmembrane proteins (Dominguez *et al.*, 1998). The antiserum previously used recognized a peptide domain common to gp27 and p26 (hp24γ_4). Furthermore, the immunofluorescence signal of endogenous proteins was below the detection limit. We therefore raised antibodies specifically recognizing the cytoplasmic domain of gp27 with high efficiency (see MATERIALS AND METHODS). This enabled us to study gp27 and to determine its precise localization in the cell.

The predominant immunofluorescence pattern of gp27 obtained using the cytoplasmic domain antibody in tissue culture cells consisted of a juxtanuclear staining coinciding with the Golgi apparatus. Figure 1 shows the comparison between gp27 and three Golgi-localized proteins: KDEL receptor (CGN and *cis*-Golgi; Griffiths *et al.*, 1994; Tang *et al.*, 1997), NAGT I (medial- and *trans*-Golgi; Dunphy *et al.*, 1985; Nilsson *et al.*, 1993), and GalT (*trans*-Golgi and *trans*-Golgi network [TGN]; Roth and Berger, 1982; Rabouille *et al.*, 1995). Single optical sections were recorded simultaneously by confocal laser-scanning microscopy and overlaid to reveal extent of colocalization (Figure 1, right panel). As can be seen, although images for gp27 and GalT were superficially similar, overlay of optical sections revealed that these proteins were segregated to a high degree. Especially foci of GalT staining were devoid of gp27. Staining for the medial- and *trans*-Golgi enzyme NAGT I and gp27 was more similar but again shifted against each other. Neither GalT nor NAGT I showed any punctate structures in the cytoplasm as seen with gp27. In contrast, the distribution of KDEL receptor was very similar to gp27, albeit somewhat stronger than gp27 in the peripheral structures and weaker in the juxtanuclear Golgi region. This suggested a *cis* localization of gp27, and to confirm this at the ultrastructural level, thawed cryosections were incubated with antibodies to gp27 and GalT. As can be seen in Figure 2a, a polarized labeling for gp27 was obtained showing labeling over both vesiculotubular profiles in close proximity to the Golgi stack as well as the first cisterna of the stack. That this corresponded to the CGN and the *cis*-cisternae, respectively, was confirmed in double-labeling experiments using GalT antibodies to label the *trans*-Golgi and the TGN. As can be seen in Figure 2b, a clear opposed labeling pattern was observed showing that gp27 resided in the CGN and the *cis*-cisterna of the Golgi apparatus.

Partial Localization of gp27 to Coated ER–Golgi Transport Structures

Having established the steady-state distribution of gp27, we next examined the nature of the peripheral structures positive for gp27 seen in addition to the juxtanuclear Golgi staining. The similar distribution of gp27 to the KDEL receptor (Figure 1) suggested that perhaps gp27 was leaving the ER en route to the Golgi apparatus and/or that it was being recycled from the Golgi apparatus. To test this, we compared the labeling of gp27 with the two sets of coats implicated in forward transport (COPI and COPII) and retrograde transport (COPI). As can be seen in Figure 3, comparison of the distribution of gp27 with Sec13, a component of the COPII coat, yielded some colocalization, especially of larger punctate structures close to the Golgi region (Figure 3, inset). However, several structures also labeled exclusively for Sec13 or gp27. Double immunofluorescence of gp27 and β′-COP, a COPI component, gave a similar picture: some structures

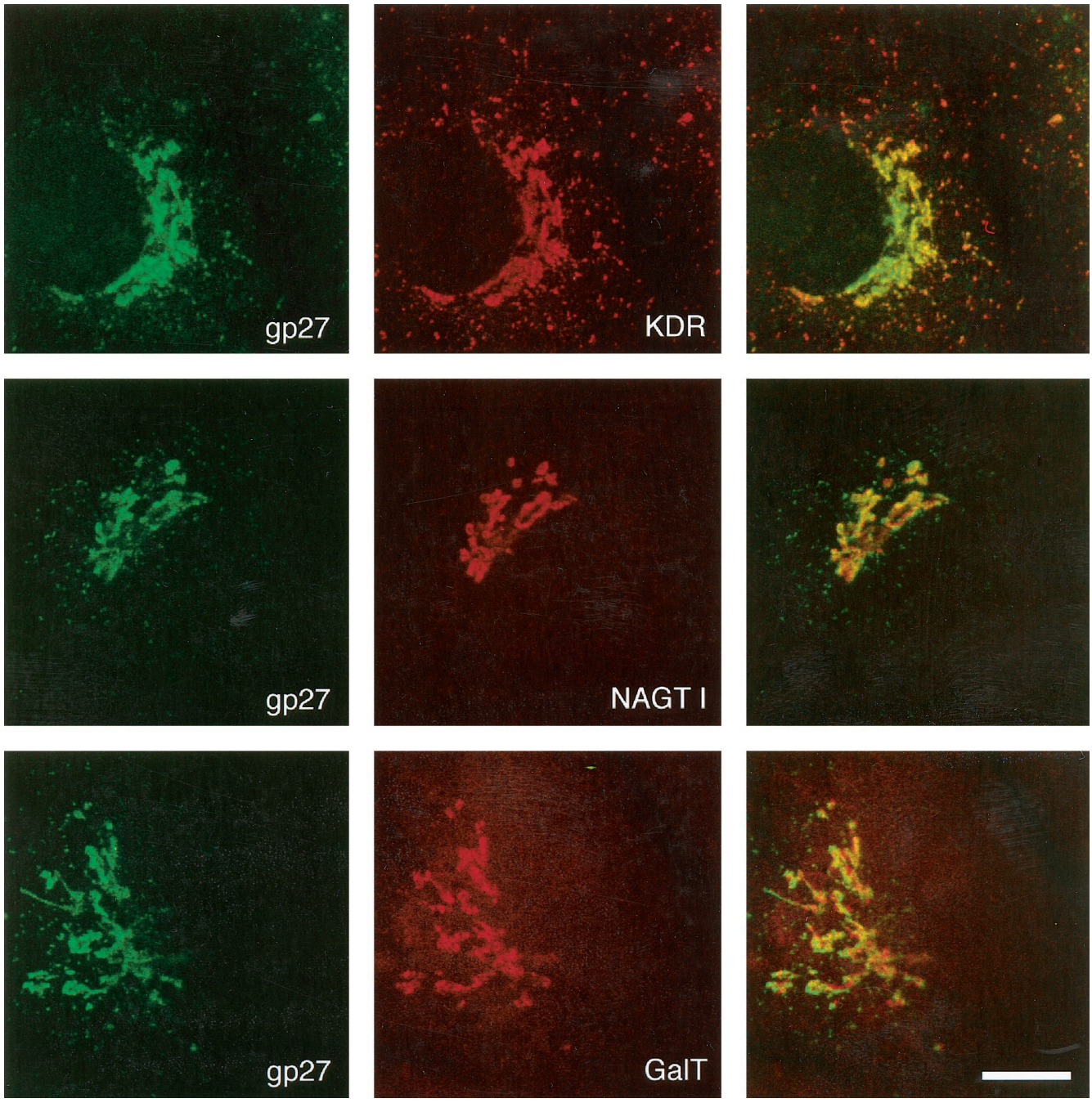

Figure 1. Comparison between gp27 and Golgi marker proteins. Double immunofluorescence stainings of Vero cells were analyzed by confocal laser scanning microscopy. Marker proteins were chosen to represent subcompartments of the Golgi apparatus: KDEL receptor for CGN and *cis*-Golgi, NAGT I for medial-Golgi, and GalT (GTL2 antibody) for *trans*-Golgi and TGN. Note that the localization of KDEL receptor and gp27 is very similar, although intensities are different. NAGT I and, even more, GalT show Golgi patterns shifted against gp27. Bar, 10 μm.

labeled for both proteins (Figure 3, inset), but the majority of staining was exclusively for either β'-COP or gp27. The direct comparison between Sec13 and β'-COP showed that both antigens were closely associated, sometimes overlapping. Taken together, these data show that gp27 exists in peripheral structures positive for both COPI and COPII, suggesting that gp27 is subjected to recycling between the Golgi apparatus and the ER. It is likely that gp27 was also present in structures negative for both COPI and

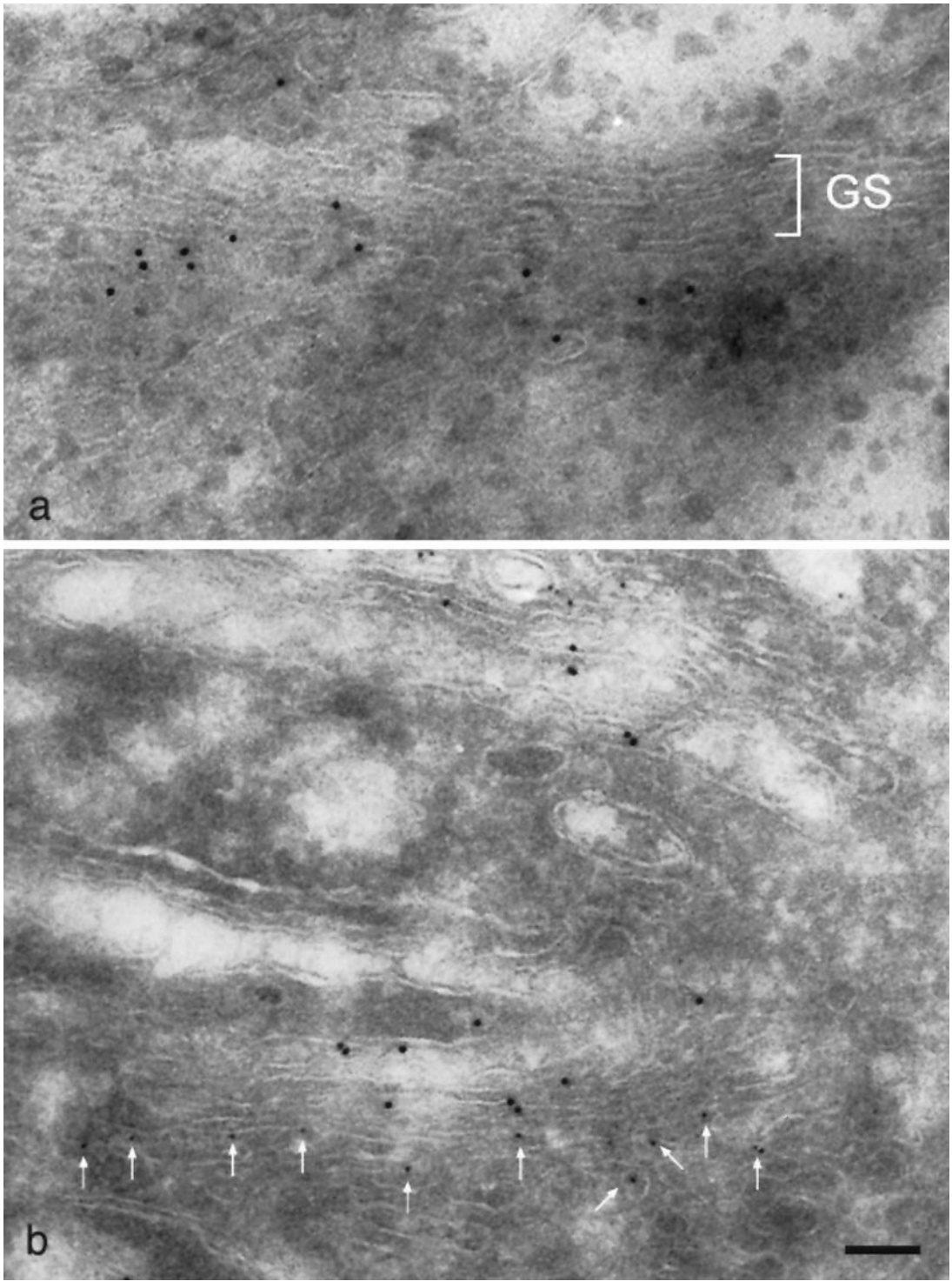

Figure 2. Ultrastructural localization of gp27 to the *cis* side of the Golgi apparatus. (a) Single labeling of HeLa cells with gp27 followed by protein A-colloidal gold (10 nm). Golgi stacks (GS) usually comprise three cisternae, and labeling for gp27 is highly polarized. (b) Comparison between the *trans*-Golgi marker protein GalT (10 nm, rabbit antiserum N10) and gp27 (5 nm). Segregation between these two proteins identifies the gp27-containing cisternae as *cis*-Golgi. Bar, 100 nm.

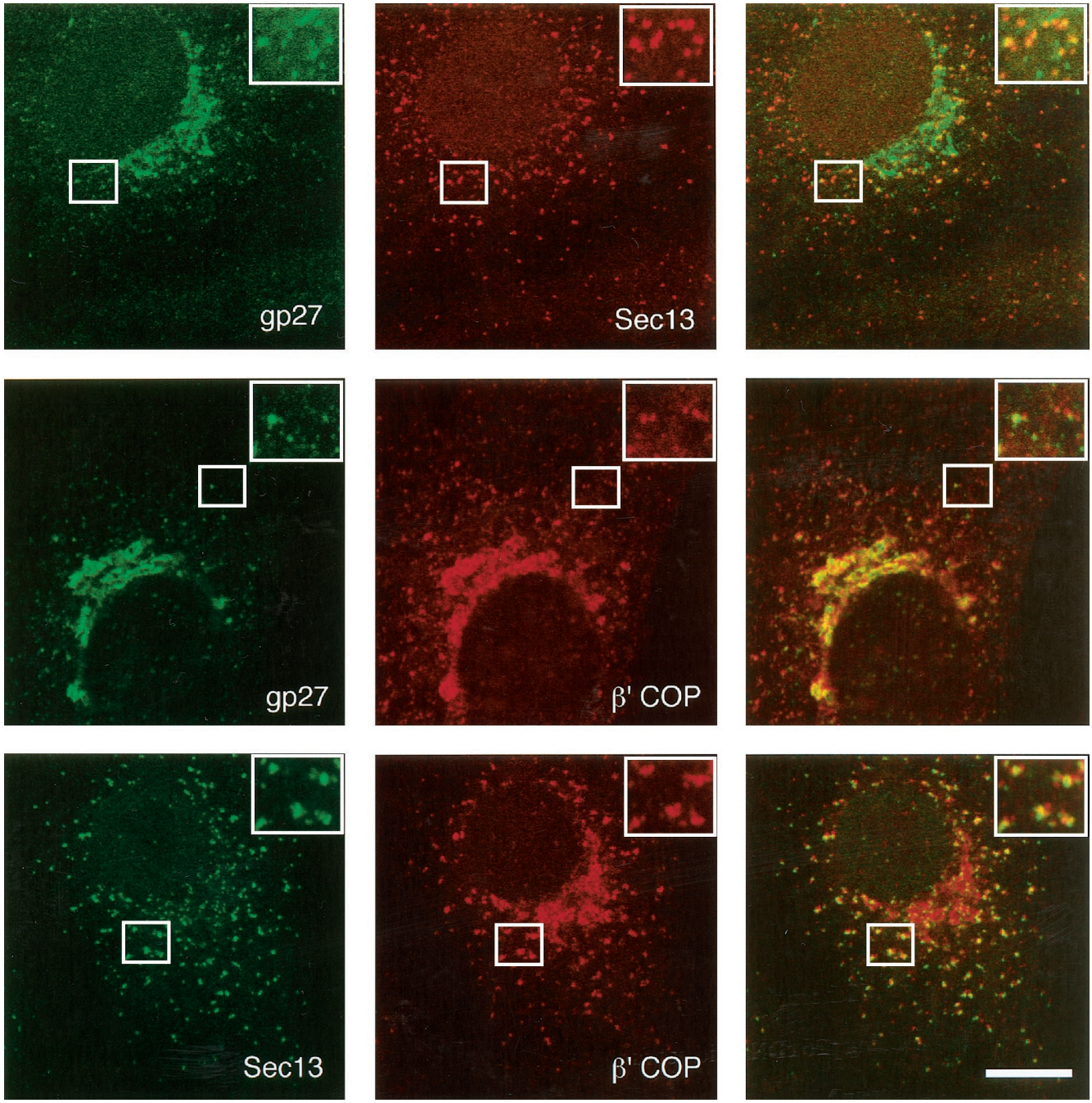

Figure 3. Localization of gp27 to coated transport structures between ER and Golgi. Double immunofluorescence stainings of Vero cells were analyzed by confocal laser-scanning microscopy. Sec13/COPII and β′-COP/COPI show some coincident staining with gp27, which is more evident in the insets. For comparison, the much more obvious closely associated staining between COPII and COPI is shown in the lower panel. Bar, 10 μm.

COPII. Future labeling experiments allowing for triple labeling will be required to examine this. However, it is also likely that gp27 may exist in structures formed by either coat but, subsequently, that such structures are uncoated.

Recycling of gp27 from the cis Side of the Golgi Apparatus to the ER and ERGIC

To examine the extent of recycling of gp27, we subjected cells to a 15°C temperature block. This treat-

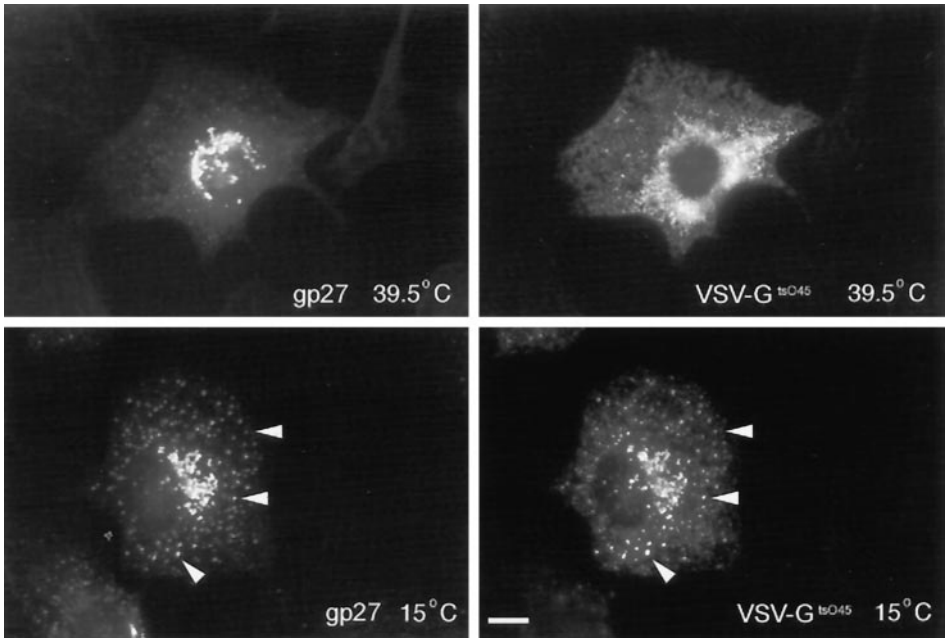

Figure 4. Accumulation of gp27 in the ER–Golgi 15°C compartment. Vero cells were infected with VSV-G^{ts045} and kept for 3 h at the restrictive temperature. After addition of the protein synthesis inhibitor cycloheximide, cells were further incubated for 1 h at 15°C. Peripheral structures of gp27 grew in number and apparent size. Note the high degree of coincident staining with VSV-G^{ts045} glycoprotein arrested on its way from ER to the Golgi apparatus. Bar, 10 μm.

ment originally led to the discovery of the ERGIC and has since been used to trap forward moving cargo together with recycling proteins of the Golgi apparatus. As an anterograde marker, we used the well-characterized and temperature-sensitive G protein of VSV, VSV-G^{ts045}. This mutant accumulates in the ER at the restrictive temperature (39.5°C). At the permissive temperature (32°C), VSV-G^{ts045} is transported out of the ER, and this also occurs at 15°C. However, in the latter, VSV-G^{ts045} is subsequently trapped in the ERGIC. As can be seen in Figure 4, shifting from restrictive temperature to 15°C caused accumulation from a previously ER-like distribution of VSV-G^{ts04} into a punctate staining pattern. These structures were confirmed to be the ERGIC by costaining for the well-characterized ERGIC marker p53 (our unpublished results). A similar if not identical staining pattern as that of the VSV-G^{ts045} was also observed with gp27 at 15°C (Figure 4, lower panel), showing that gp27 has relocated from the *cis* side of the Golgi into the ERGIC. Recycling of gp27 was further confirmed by subjecting cells to the fungal metabolite brefeldin A. Brefeldin A is known to cause a dramatic redistribution of Golgi-resident glycosylation enzymes to the ER. By comparison, p53 of the ERGIC and the KDEL receptor accumulate in tubulovesicular clusters scattered throughout the cytoplasm. These peripheral structures are morphologically and biochemically distinct from the brefeldin A–induced ER–Golgi hybrid (Füllekrug *et al.*, 1997), and accumulation of proteins into these peripheral structures serve as a good indication for recycling from the Golgi apparatus. As can be seen in Figure 5, brefeldin A treatment of cells caused gp27 to redistribute into peripheral structures colocalizing well with the KDEL receptor. In contrast, the medial- and *trans*-glycosylation enzyme NAGT I gave as expected a reticular staining pattern consistent with an ER distribution. The accumulation of gp27 into peripheral structures further supported the notion that gp27 recycles. Colocalization with Sec13 after brefeldin A treatment can also be used as a criteria for recycling. This was shown in studies examining redistribution of the KDEL receptor upon brefeldin A treatment, which revealed a dramatic increase in peripheral structures colocalizing with Sec13 (Tang *et al.*, 1997). As can be seen in Figure 5, labeling for Sec13 revealed an extensive colocalization with gp27 upon brefeldin A treatment. This colocalization was significantly higher than that observed in control cells (Figure 3). As a further test for gp27 recycling, the effect of microinjection of cells with the dominant negative mutant of Sar1 (Sar1p^{dn}), a small GTPase needed for export out of the ER, was determined. As can be seen in Figure 6, microinjection of Sar1p^{dn} in the presence of emetine (an effective inhibitor of protein synthesis) resulted in a gradual ER accumulation of gp27, showing that gp27 recycles through the ER. However, the ER accumulation of gp27 was relatively low even after 3 h, indicating that the extent of recycling was slower than that expected for recycling proteins such as ERGIC53 (Shima *et al.*, 1998). The ER accumulation of gp27 (Figure 6) was more comparable with that of the Golgi glycosylation enzyme *N*-acetylgalactosaminyltransferase-2 under the same conditions (Storrie *et al.*, 1998). In conclusion, these data show that gp27 recycles extensively from the *cis* side of the Golgi appara-

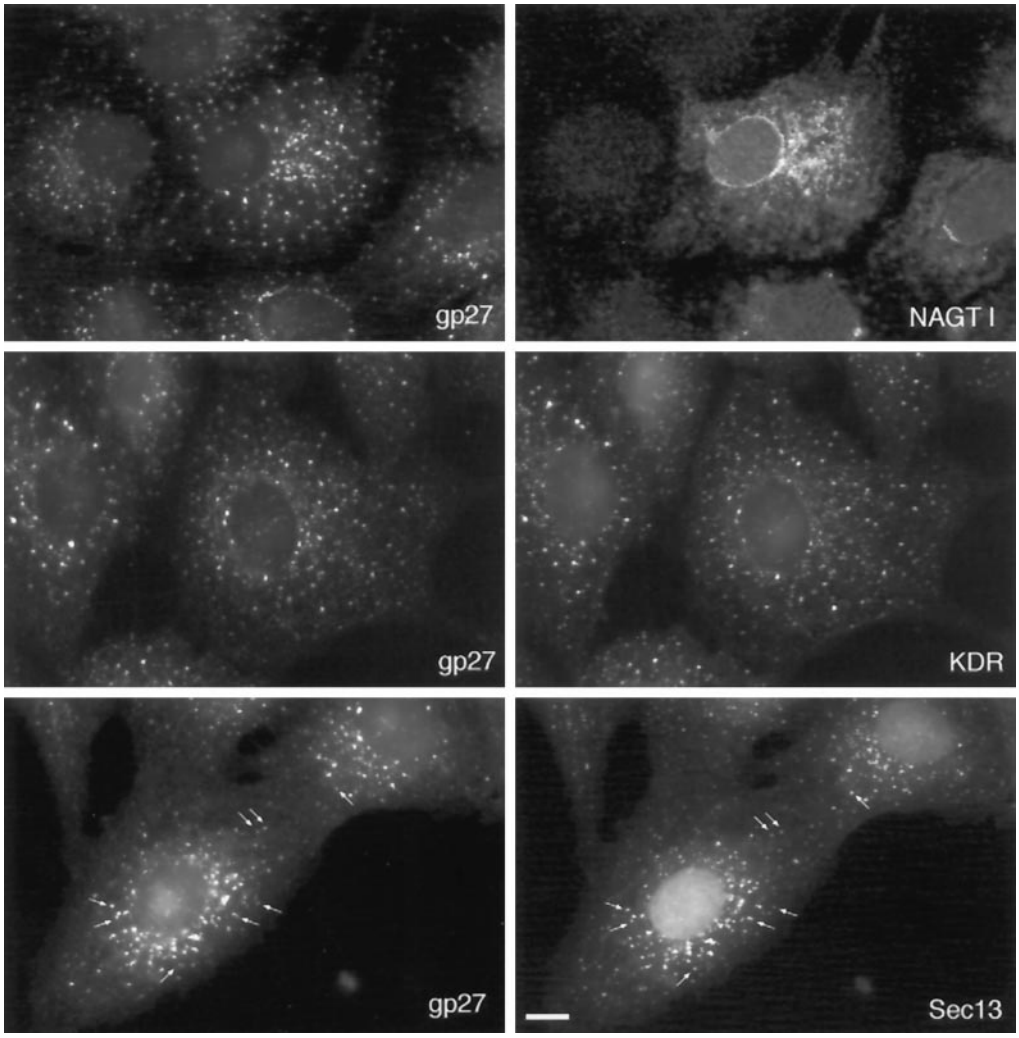

Figure 5. Subcellular distribution of gp27 after brefeldin A treatment. Resident glycosylation enzymes such as NAGT I stain nuclear envelope and reticular cytoplasmic ER structures, but gp27 distribution is different. A striking coincidence of staining is observed with KDEL receptor, and many of the brefeldin A–induced punctated structures are coincident with Sec13/COPII. Bar, 10 μm.

tus. Presumably, such recycling is part of the mechanism for maintaining its steady-state distribution. Also, it may reflect a functional aspect, perhaps to allow it to interact with other p24 proteins. To test for the latter, we examined whether gp27 complexed with other p24 proteins.

gp27 Is Part of a Complex Containing Other p24 Family Proteins

With the new antibodies recognizing specifically the cytoplasmic domains of the native gp27 and p26, we were able to directly examine the interactions between p24 proteins. Figure 7a shows a representative coimmunoprecipitation experiment. An immunoprecipitation with gp27 antibody of a metabolically labeled lysate prepared in the presence of SDS yielded one prominent band at 30 kDa (Figure 7a, A), which corresponds to the molecular mass observed for gp27 upon Western blotting and immunodetection. Under nondenaturing conditions we observed two additional bands, one at 28 kDa (Figure 7a, B) and one at 22 kDa (Figure 7a, C), the latter one being the strongest of the three bands. 2D gel electrophoresis resolved these bands into five individual spots (Figure 7a, A1, A2, B, C1, and C2). The ^{35}S-labeled immunoprecipitate was mixed with an unlabeled Golgi-enriched fraction and probed with antibodies against p24 family proteins by Western blotting. All five spots were identified by comparing films obtained from radioactive material (Figure 7a) and immunodetection (Figure 7b). A1 and A2 are identical to gp27, with A1 corresponding to an uncharged isoform and A2 to a sialylated form of gp27

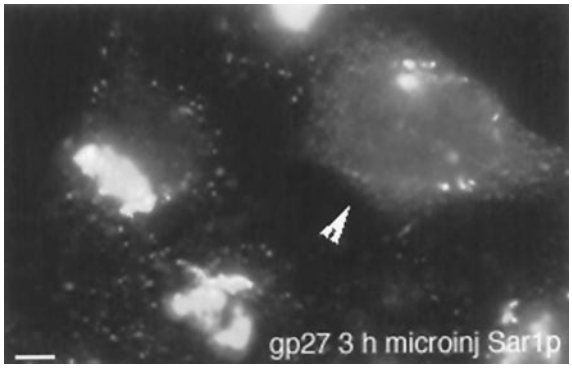

Figure 6. Microinjection of Sar1p^{dn} to block ER export leads to a slow accumulation by 3 h of gp27 in the ER. HeLa cells were microinjected with Sar1p^{dn} in the presence of 5 μg/ml emetine to inhibit protein synthesis. Cells were then incubated for 3 h at 37°C in complete media in the presence of emetine. Cells were fixed with formaldehyde and immunofluorescently labeled for gp27. The arrowhead points to the microinjected cell in this example field. Note that a juxtanuclear gp27 staining pattern of noninjected control cells is largely absent in the microinjected cell. Considerable diffuse cytoplasmic fluorescence indicative of ER localization is present in the injected cell. Bar, 10 μm.

(see below). B corresponds to GMP25, C1 to p23, and C2 to p24. The strongest labeled spot was always C2/p24, which contains 10 methionine residues per molecule compared with only two for every gp27 molecule. Quantification and correction for methionine content (Table 1) argued that p23, p24, and GMP25 were coprecipitated with gp27 in similar amounts, suggesting an equimolar representation. The composition of this complex was confirmed using antibodies against p23 (Table 2). Depending on the respective antibodies used, gp27 and p23 were present in higher amounts than the coprecipated p24 family proteins. On the other hand, comparison of gp27 with p24 and GMP25 in the immunoprecipitate obtained with p23 antibodies (or comparing p23 with p24 and GMP25 in the gp27 immunoprecipitate) indicated approximately similar molar amounts. Only GMP25 was found at higher levels, which could indicate a preferential subcomplex formation between p23 and GMP25. In principal there are two possible reasons for partial participation in complex formation: either only a fraction of each p24 family protein is in the complex, or our conditions for immunoprecipitation were not sufficient to preserve hetero-oligomeric structures completely. That the revealed coprecipitation was not a consequence of a detergent-insoluble or nonspecific protein aggregation was tested for. Under the conditions used, caveolin, a marker for the CGN/*cis*-cisternae (Parton, personal communication) as well as in the TGN and on the plasma membrane (Dupree *et al.*, 1993), was found in the detergent-insoluble pellet (Figure 7, inset, P), whereas gp27 was efficiently solubilized (Figure 7, inset, S).

Much to our surprise, affinity-purified p26 antibodies did not coprecipitate any other known p24 family proteins (Table 2). Instead, only two major proteins were found on 2D gels, one of them being p26 and the other one a so far unidentified protein (pX). This showed that complex formation was specific for particular p24 proteins.

Some additional spots of higher molecular mass were also apparent (Figure 7, a and c). These correspond to unspecific contaminants, because they were also seen in mock immunoprecipitations using preimmune serum (Figure 7, inset) or rabbit IgG. Judged by isoelectric point and molecular mass, actin and α- and β-tubulin are likely to be among them.

Other human p24 family proteins have been described (T1/ST2R-BP; Gayle *et al.*, 1996) or assembled from expressed sequence tags (atp20; our unpublished data). These proteins have a calculated molecular mass and isoelectric point that are in the range of the 2D gel of Figure 7. Table 1 shows a back-calculation assuming these two p24 family proteins would be present in a molar amount similar to p23, p24, or GMP25 in gp27 immunoprecipitates. Spots with these counts would have been impossible to miss under our conditions. This means that either these proteins are not present in the hetero-oligomeric structure or they are not expressed in HeLa cells. Interestingly, gp27, p26, T1/ST2R-BP, and atp20 all belong to the γ branch of the p24 family tree (Dominguez *et al.*, 1998). This would indicate that only one member of this class is present in the hetero-oligomeric complex brought down using either the antibody to gp27 or p23.

Coexpression of p24 Family Proteins Is Essential for Export of gp27 from the ER

We next examined whether complex formation might be required for ER export of gp27. To allow for identification of expressed as opposed to endogenous gp27, we introduced an epitope tag, VSV-G, at the extreme N terminus of the mature protein. To increase expression, we substituted the signal sequence with that of CD8. The resulting cDNA encoded a VSV-G–tagged gp27, which showed no signs of differential behavior compared with the wild-type gp27 in independent control experiments. Microinjection of the non-tagged cDNA inserted into pCMUIV into HeLa cells produced a distinct ER-like pattern (our unpublished observation), as seen with the VSV-G–tagged gp27 when expressed alone (see below). Also, expression of the VSV-G–tagged lumenal domain of gp27 fused to the transmembrane and cytoplasmic domain of CD8 shows that this hybrid molecule is not arrested in the ER but is efficiently transported to the plasma membrane (our unpublished observation).

Expression of this tagged gp27 in HeLa cells and analysis of subcellular localization by immunofluorescence

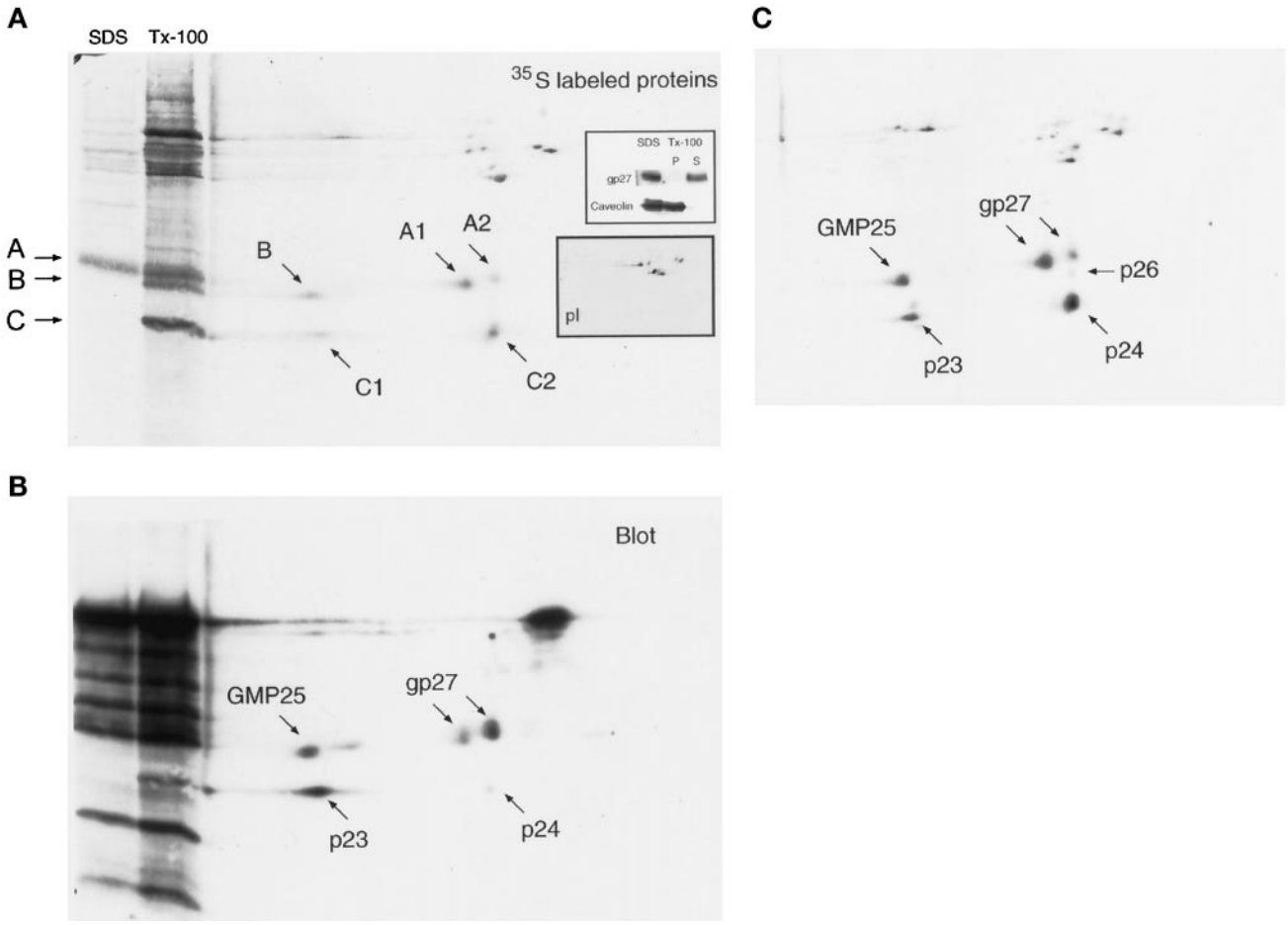

Figure 7. Coimmunoprecipitation of p24 family proteins with gp27 affinity-purified antibodies. [^{35}S]Methionine was used for labeling HeLa cells overnight, and lysis was routinely done with the nonionic detergent TX-100. Under these conditions, gp27 was efficiently solubilized (a, inset; p, pellet; S, supernatant), whereas large detergent-resistant structures containing caveolin, a protein residing mostly in the CGN and the *cis*-Golgi as well as on plasma membrane (Dupree *et al.*, 1993; Parton, personal communication), were sedimented and would not be present in the starting lysate for immunoprecipitation. Immunoprecipitates obtained with gp27 antibodies were analyzed by 1D SDS-PAGE (a, lanes SDS and TX-100) and isoelectric focusing followed by SDS-PAGE (a–c). Under denaturing conditions (a, SDS), one prominent band at 30 kDa corresponding to gp27 is resolved. Using TX-100 (b, Tx-100), three major bands in the 20- to 30-kDa range were observed (A–C). 2D gel analysis resolved this pattern into five different spots: A1, A2, B, C1, and C2 (a). The same 2D gel loaded with ^{35}S-labeled immunoprecipitate and unlabeled Golgi-enriched subcellular fraction is shown in a and b. After detection of radioactively labeled proteins (a), the membrane was probed with antibodies against p24 family proteins (b). Alignment of the two patterns identified coprecipitated proteins as different p24 family members. Protein A-peroxidase was applied for detection of primary antibodies against p24 family proteins, which also bound to IgGs of the gp27 antibodies used for immunoprecipitation, giving rise to the additional strong staining patterns apparent in b. Some additional spots of higher molecular mass are also apparent and are likely to be unspecific contaminants, because they are also seen when using preimmune serum (pI) or rabbit IgG (a, inset). 2D gels loaded with labeled immunoprecipitate without added Golgi fraction were of sufficient resolution to enable quantification (c).

are shown in Figure 8. Expressed on its own, gp27 localized to the ER except for a few cells, which also showed Golgi staining. Biochemical analysis demonstrated that it stayed Endo H sensitive and was degraded (our unpublished results). Coexpression with p23 led to some export of gp27 out of the ER. Interestingly, under these conditions, Golgi retention seemed to be impaired, because gp27 was also found at the plasma membrane and in lysosomal structures. Coexpression with p24 gave rise to large pleiomorphic clusters. These structures were also seen in other cotransfections but were most prominent when coexpressing p24 and gp27. In terms of conferring Golgi localization, coexpression of the two closely related p24 family members gp27 and p26 was the least effective combination. In some triple transfections (gp27 + p23 + p24 and gp27 + p23 + GMP25) the portion of cells displaying Golgi staining was higher than in any of the double transfections but was almost always accompanied by ER staining and pleiomorphic clusters. Only the cotransfection using gp27, p23, p24, and GMP25

Table 1. Quantification of immunoprecipitated proteins using gp27

	Count	Count, (−background)	Methione (mature protein)	Count, (−background)/Met	%
gp27 (0)	20,913	20,885	2	10,443	41.7
gp27 (−1)	7,651	7,623	2	3,812	15.2
gp27 (0,−1)	28,564	28,508	2	14,255	56.9
p23	18,140	18,112	5	3,622	14.5
p24	29,720	29,692	10	2,969	11.9
GMP25	13,531	13,503	4	3,376	13.5
p26	1,656	1,628	2	814	3.3
Background	28	0			
T1/ST2R-BP	10,000		4	2,500	10
atp20	17,500		7	2,500	10

[^{35}S]Methionine was used for labeling HeLa cells overnight, and immunoprecipitates were analysed by 2D gel electrophoresis. The PhosphorImager system was used for quantification. Counts for both forms of gp27 were combined [gp27(0) = uncharged; gp27(−1) = negatively charged]. The background area was chosen to lie in the middle of the p24 family proteins. After subtraction of background, the count value was divided by the number of methionine residues present in the respective mature (without signal sequence) p24 family proteins. This enabled comparison on a molar basis, assuming that incorporation of methionine was equally efficient at every position. Of all the immunoprecipitated p24 family proteins, gp27 constituted 56.9%. Values for p23, p24, and GMP25 ranged from 11.9 to 14.5%, but the amount of p26 was significantly lower (3.25%). The rows for T1/ST2R-BP and atp20 show a back-calculation assuming they would be present in an amount similar to p23, p24 or GMP25. Spots corresponding to the counts predicted by this calculation were not observed, although these two p24 family members would be well within the analysed molecular weight and isoelectric point.

gave a convincing perinuclear Golgi pattern. Other staining patterns were also observed, which are most likely due to the variability in the expression of the individual cDNAs. Such variations in expression levels of the different p24s could indicate limitations of this approach. However, we routinely observed comparable expression levels of the VSV-G–tagged gp27 in the different combinations used, arguing that the observed inability of gp27 to leave the ER in the absence of the other p24 members was not a consequence of increased expression per se. Adding p26 cDNA did not further improve the situation in terms of Golgi localization (our unpublished results).

Taken together, these experiments suggest that coexpression is required for efficient export of newly synthesized p24 family proteins out of the ER. This could point toward a requirement for heterotypic complex formation for gp27 to leave the ER. In separate experiments, we examined whether a requirement for coexpression was specific only for gp27. All other p24 family proteins tested behaved similarly, showing a direct need for complex formation in ER export localization (our unpublished results).

Differential Glycosylation of gp27 and GMP25 Suggests Alternate Routes of Recycling

Having established that a portion of gp27 forms a complex with GMP25, p23, and p24, we compared the

Table 2. Quantification of immunoprecipitated proteins using antibodies against gp27, p23, and p26

	gp27 Ip count	gp27 Ip (%)	p23 Ip count	p23 Ip (%)	p26 Ip count
gp27 (0,−1)	144,855	68	12,306	10	
p23	50,811	9.5	99,580	53	
p24	77,187	7.3	40,212	10	
GMP25	64,629	15	41,088	26	
p26					70,461
pX					43,022
Background	941		2,556		7,644

All immunoprecipitations (Ip) were done with the same lysate. Although the coprecipitation using gp27 antibodies in this case was less efficient for p23 and p24 compared with Figure 7C, counts were still high above background. In the area corresponding to p26, no signal above background was observed. Note that p23 also coprecipitates three other p24 family proteins: gp27, p24, and GMP25. Immunoprecipitation with p26 antibodies did not give any signal in the areas corresponding to gp27, p23, p24, or GMP25. Instead, a protein (pX) with an isoelectric point close to p26 was coprecipitated. Because the methionine content of this protein is unknown, no further calculation is possible. Blank spaces in the table represent no significant counts above background.

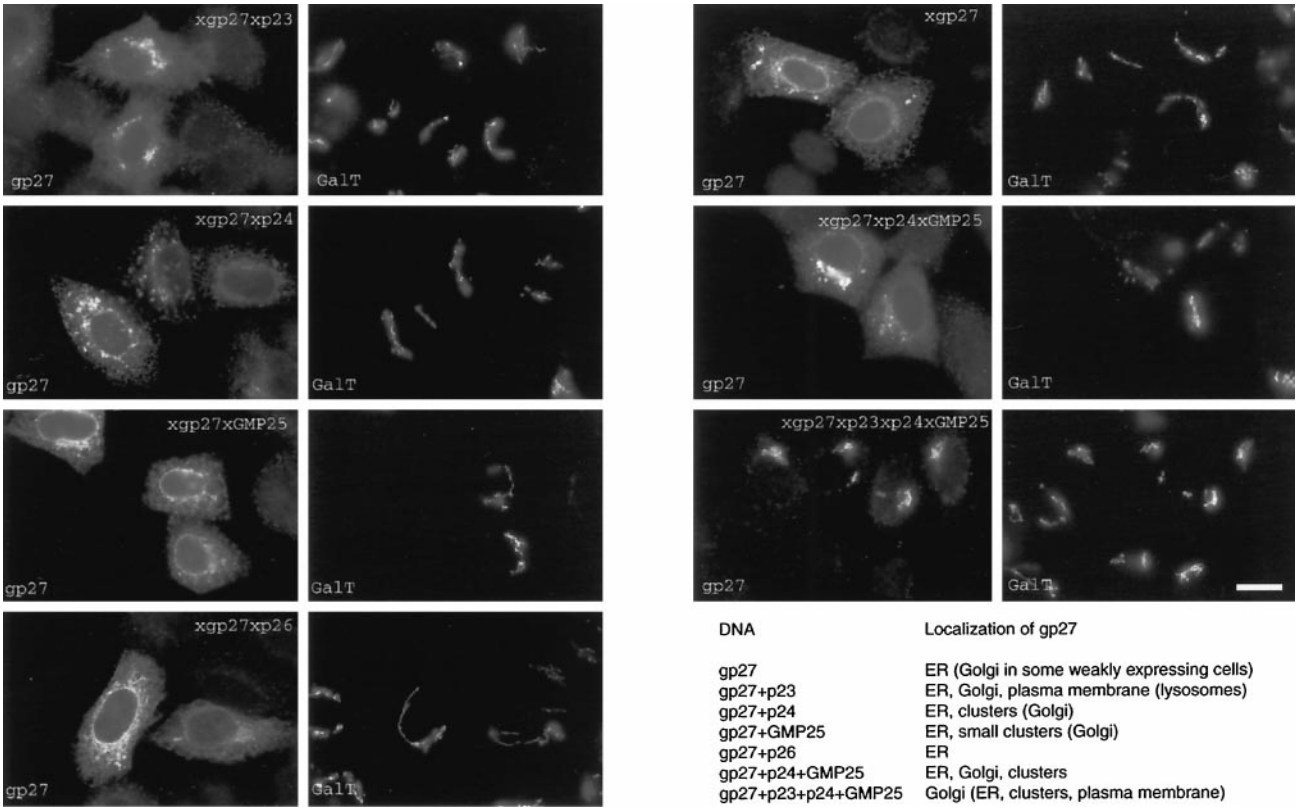

Figure 8. Coexpression of p24 family proteins allows transport of gp27 from ER to the Golgi apparatus. HeLa cells were transiently transfected with gp27 cDNA (20%) and other p24 family cDNAs (20% each, pcDNA3 vector DNA making up to 100%). The Golgi apparatus was identified by mAb GTL2 against GalT. Without coexpressed p24 proteins, the predominant staining pattern for overexpressed gp27 is ER. Double transfection of gp27 with other p24 family cDNAs gives different phenotypes depending on which particular cDNA is used. In terms of Golgi localization, coexpression of p23, p24, and p25 is the most efficient combination. See table and text for details. The localization indicated in parentheses in the table is not the predominant phenotype but was observed consistently. Bar, 10 μm.

degree of glycosylation of gp27 and GMP25 in HeLa cells. Sequence analysis of gp27 predicts a consensus site for N-linked glycosylation. Peptide *N*-glycanase F digestion confirmed that gp27 is a glycoprotein (Figure 9). Further characterization revealed resistance to Endo H, indicating that gp27 was modified by glycosylation enzymes of the medial- and *trans*-Golgi. This was in contrast to GMP25, which remained Endo H sensitive (Figure 9), at steady state. Further analysis by neuraminidase digestion and 2D gel analysis showed that gp27 displayed not only complex oligosaccharides but also terminal ones in the form of sialic acid. In fact, at steady state, the predominant form carried one sialic acid (see Figure 7b). Kinetic analysis showed further that gp27 acquired Endo H resistance, with a $t_{1/2}$ of ~50 min, whereas sialylation took much longer. After overnight labeling for 15 h, uncharged gp27(0) was still the predominant form [73 vs. 27% of gp27(−1)]. After 20 h, both species were present in the same amount [51% of gp27(0) vs. 49% of gp27(−1)]. This shows that gp27 has a long half-life and that it is slowly but gradually converted into a glycoprotein displaying complex and terminal oligosaccharides. This gradual conversion is most consistent with a recycling behavior and fully consistent with the observations presented above. That GMP25 displayed <5% complex oligosaccharides at steady state and under the same conditions as that observed for gp27 was surprising. (Table 3 summarizes the data on N-linked glycosylation of mammalian p24 family proteins.) In our previous study (Dominguez *et al.*, 1998), GMP25 was in rat liver Golgi found to be Endo H resistant at steady state.

This would indicate that GMP25 is subjected to a more extensive exposure to later modifying glycosylation enzymes, perhaps as a consequence of more extensive recycling in these highly secreting cells. In HeLa cells, very little GMP25 is converted into complex form, showing that although clearly capable of forming heterotypic complexes, they cannot share identical steady-state distributions and/or recycling routes. This argues that complex formation is a dynamic process and provides an important insight into the behavior of p24 proteins.

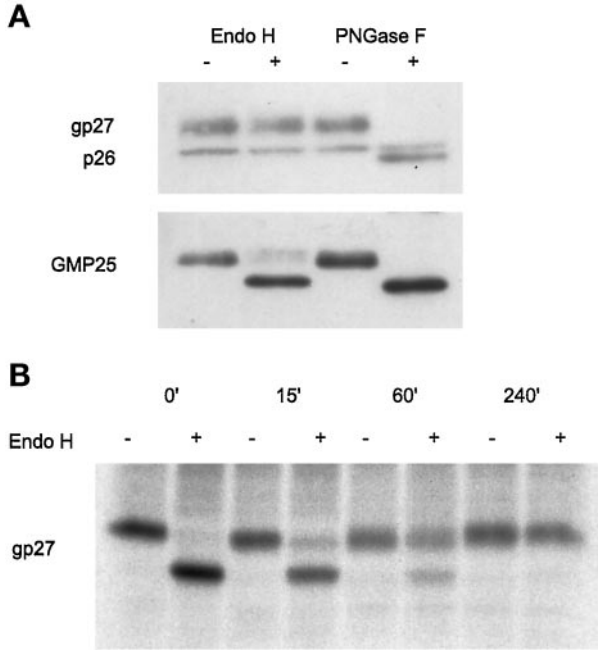

Figure 9. Glycosylation analysis of gp27 and GMP25 in HeLa cells. (a) Removal of N-linked oligosaccharides by peptide *N*-glycanase F led to faster migration of both proteins, but p26 is not affected. Maturation of the oligosaccharide chain of gp27 in the medial-Golgi renders it resistant to digestion with Endo H. The amount of Endo H–sensitive GMP25 is ≥95%. (b) Pulse–chase analysis of the acquisition of Endo H resistance for gp27. After 60 min, two-thirds of gp27 are already Endo H resistant.

DISCUSSION

We have in this study presented evidence showing that gp27 (hp24γ_3) interacts in a heterotypic manner with three other p24 proteins and that such complex formation is required for ER exit. Despite this, oligosaccharides attached to gp27 and GMP25 (hp24α_2) show different extents of modifications, arguing that they recycle differentially. We also show that at steady state, gp27 resides at the *cis* side of the Golgi apparatus from where it recycles to earlier compartments.

Steady-State Localization of gp27

We previously reported on the steady-state distribution of different p24 proteins. Subcellular fractionation showed that p24 proteins reside in membranes of intermediate-density ER corresponding well to the ERGIC marker p53/58. Indirect immunofluorescence showed typical Golgi staining patterns for all p24s with the exception of GMP25, which showed relatively more ER labeling. This was confirmed by immunoelectron microscopy, which defined the steady-state localization of GMP25 to the ER, the ERGIC, and the CGN (Dominguez *et al.*, 1998). The localization of p23 (hp24δ_1) has also been determined at the ultrastructural level and shows that p23 resides mainly in the CGN colocalizing extensively with the KDEL receptor (Rojo *et al.*, 1997). In our previous study, we were unable to distinguish between gp27 and p26 (hp24γ_4), because the antibody used was raised to a common epitope for these p24 proteins. Because gp27 and p26 share extensive homology in their lumenal domains but display quite divergent cytoplasmic domains, we raised antibodies toward the cytoplasmic domains of both gp27 and p26. Indirect immunofluorescence of gp27 revealed a compact juxtanuclear staining pattern typical of the Golgi apparatus with additional staining of peripheral small punctate structures. Double immunofluorescence of gp27 and confocal analysis gave a good colocalization with the KDEL receptor, which suggested that gp27 mainly resides in the CGN and *cis*-cisterna of the Golgi apparatus. This was confirmed at the ultrastructural level, revealing a compact and polarized labeling on the *cis* side comprising both the CGN and the *cis*-cisterna.

Recycling of gp27

The notion that gp27 also existed in peripheral structures was indicative of a recycling protein. In fact,

Table 3. Summary of N-glycosylation of p24 family proteins

Name	N-X-S/T	Cells	PNGase F sensitive	Endo H sensitive	NA sensitive	Type of N-glycosylation
p23	N179	HeLa	No	No	No	None
p24		HeLa	No	No	No	None
GMP25	N104	HeLa	Yes	Yes	No	High mannose
		Rat liver	Yes	Yes	Yes	Complex (−4,−3,−5,−2)
p26		HeLa	No	No	No	None
gp27	N90	HeLa	Yes	No	Yes	Complex (−1,0)
		Rat liver	Yes	No	Yes	Complex (−5,−6,−4)

Compared with HeLa cells, gp27 and GMP25 are apparently cycling more extensively in rat liver, and both glycoproteins are modified by sialic acid. Still, gp27 is more extensively modified than GMP25. Charged isoforms are listed in order of their relative abundance.

colocalization between gp27 and the KDEL receptor also in peripheral structures argued for very similar behavior of these two proteins. Colabeling of gp27 in some of the peripheral structures with coat proteins of COPI and COPII further suggested a routing of gp27 between the Golgi apparatus and earlier compartments. That gp27 was indeed subjected to recycling was tested for in three different ways. First, cells expressing the temperature-sensitive mutant of VSV-G^{ts045} were shifted from restrictive temperature to 15°C to accumulate this anterograde transport marker in the ERGIC (originally identified as the 15°C compartment; Saraste and Kuismanen, 1984). This showed that gp27 effectively redistributed into the ERGIC where it was then found to codistribute with the trapped anterograde cargo VSV-G^{ts045}. Second, brefeldin A treatment also supported the notion of recycling. Recycling proteins such as the KDEL receptor and p53/58 of the ERGIC both redistribute into punctate structures upon brefeldin A treatment, whereas resident glycosylation enzymes (e.g., NAGT I and GalT) effectively redistribute into the ER. Indeed, brefeldin A treatment showed that gp27 redistributed into peripheral structures in much the same way as the KDEL receptor. The nature of these structures was suggested by their labeling for the COPII component Sec13, suggesting that these peripheral structures were related or in proximity of ER exit. Microinjection of the dominant negative mutant of Sar1 ($Sar1p^{dn}$), a small GTPase needed for COPII-mediated export out of the ER, produced a slow but gradual accumulation, showing that at least a portion of gp27 recycles through the ER. The rate of accumulation of gp27 in the ER was somewhat lower than that expected for p53/58 of the ERGIC (Shima *et al.*, 1998; our unpublished results) and more consistent with the observed kinetics for the Golgi stack resident glycosylation enzyme GalNAc-T2 (Storrie *et al.*, 1998). However, this was assessed only at a qualitative level, and further work will have to be done to determine the precise recycling rate of gp27.

The slow addition of sialic acid to gp27 combined with the observation that at steady state, the bulk of gp27 is sialylated is characteristic of recycling proteins and is to be expected given the observed behavior of gp27. It also argues that gp27 has a very long half-life. Conversion into complex oligosaccharides and, later, the addition of terminal monosaccharides are the consequences of gp27 having a limited access to later compartments of the Golgi apparatus. Alternatively, gp27 is subjected to modifications of recycling glycosylation enzymes intersecting with gp27 in the *cis*-cisternae or the CGN. To distinguish between these two possibilities is at present difficult. That gp27 does recycle though is strongly supported by the above data.

Heterotypic Complex Formation of gp27 and Differential Recycling

The coimmunoprecipitation of p23, p24 (hp24β_1), and GMP25 with gp27 shows that these proteins form a hetero-oligomeric complex. It is unlikely that this complex is the result of an unspecific aggregation of transmembrane proteins sharing physicochemical properties. The best evidence for specificity was provided by immunoprecipitation experiments of p26. Such immunoprecipitation experiments did not result in the coimmunoprecipitation of p23, p24, or GMP25. Furthermore, very little p26 was observed to coprecipitate with gp27. There exists precedence for heterotypic interactions between p24 proteins in yeast. Both emp24 (yp24β_1) and erv25 (yp24δ) coprecipitate after chemical crosslinking (Belden and Barlowe, 1996). The apparent equimolar representation of p23, p24, and GMP25 in the heterotypic complex with gp27 suggests that this complex formation is of functional significance. Where such complex formation exists at steady state is at present difficult to determine. Although there exists a clear requirement for complex formation of the p24 proteins in the ER, as shown by the need for coexpression, this does not rule out complex formation beyond the ER. In fact, the slow but gradual ER accumulation of gp27 in the ER upon blocking ER export suggests that gp27 does not recycle rapidly through the ER. Instead, complex formation may initially take place in the ER, but subcomplexes may then exist in dynamic equilibrium in the CGN and the *cis*-cisterna. The observation that ~15% of gp27 participated in the complex may also be a reflection of a loss of material during the coprecipitation procedure. This we consider unlikely, because gp27 and GMP25 display oligosaccharides of different maturity, gp27 being Endo H resistant and GMP25 Endo H sensitive, at steady state. This makes it unlikely that these two p24 proteins exist in a stable complex at all time. Rather, we suggest that the identified complex exists in a dynamic equilibrium.

The notion that gp27 recycles and that it exist in a complex with other p24 proteins provides a novel insight into the behavior of this family. Their abundance and high degree of conservation between species argues for a fundamental role for p24 proteins in the early secretory pathway. We favor the idea that through their ability to bind to each other as well as to coat proteins, they serve both a structural as well as functional role in the maintenance of the ER-to-Golgi transport pathway.

Note Added in Proof. Please also see the work by Marzioch *et al*. (1999; this issue) for further evidence for complex formation of p24 proteins in yeast.

ACKNOWLEDGMENTS

We gratefully acknowledge the kind gifts of reagents from Eric G. Berger, Bill Balch, Kai Simons, and Hans-Dieter Söling. The TCS-NT confocal laser scan microscope was provided by Leica Lasertechnique (Heidelberg, Germany) as an active participant in the Advanced Light Microscopy Facility at EMBL. We are especially grateful to Alan Sawyer (EMBL) for help with hybridoma cell lines and Sigrun Brendel (EMBL) for the preparation of ultrathin cryosections. This work was supported by Deutsche Forschungsgemeinschaft long-term fellowship Fu 340/1-1 (to J.F.). B.S. was supported by a grant from the Fogarty International Center of the US National Institutes of Health.

REFERENCES

Aridor, M., Bannykh, S.I., Rowe, T., and Balch, W.E. (1995). Sequential coupling between COPII and COPI vesicle coats in endoplasmic reticulum to Golgi transport. J. Cell Biol. *131*, 875–893.

Belden, W.J., and Barlowe, C. (1996). Erv25p, a component of COPII-coated vesicles, forms a complex with Emp24p that is required for efficient endoplasmic reticulum to Golgi transport. J. Biol. Chem. *271*, 26939–26946.

Blum, R., Feick, P., Puype, M., Vandekerckhove, J., Klengel, R., Nastainczyk, W., and Schulz, I. (1996). Tmp21 and p24A, two type I proteins enriched in pancreatic microsomal membranes, are members of a protein family involved in vesicular trafficking. J. Biol. Chem. *271*, 17183–17189.

Dominguez, M., Dejgaard, K., Füllekrug, J., Dahan, S., Fazel, A., Paccaud, J.P., Thomas, D.Y., Bergeron, J.J., and Nilsson, T. (1998). gp25L/emp24/p24 protein family members of the *cis*-Golgi network bind both COP I and II coatomer. J. Cell Biol. *140*, 751–765.

Dunphy, W.G., Brands, R., and Rothman, J.E. (1985). Attachment of terminal *N*-acetylglucosamine to asparagine-linked oligosaccharides occurs in central cisternae of the Golgi stack. Cell *40*, 463–472.

Dupree, P., Parton, R.G., Raposo, G., Kurzchalia, T.V., and Simons, K. (1993). Caveolae and sorting in the *trans*-Golgi network of epithelial cells. EMBO J. *12*, 1597–1605.

Elrod-Erickson, M.J., and Kaiser, C.A. (1996). Genes that control the fidelity of endoplasmic reticulum to Golgi transport identified as suppressors of vesicle budding mutations. Mol. Biol. Cell *7*, 1043–1058.

Evan, G.I., Lewis, G.K., Ramsay, G., and Bishop, J.M. (1985). Isolation of monoclonal antibodies specific for human c-myc proto-oncogene product. Mol. Cell. Biol. *5*, 3610–3616.

Füllekrug, J., Sönnichsen, B., Schäfer, U., Nguyen Van, P., Söling, H.D., and Mieskes, G. (1997). Characterization of brefeldin A induced vesicular structures containing cycling proteins of the intermediate compartment/*cis*-Golgi network. FEBS Lett. *404*, 75–81.

Gayle, M.A., Slack, J.L., Bonnert, T.P., Renshaw, B.R., Sonoda, G., Taguchi, T., Testa, J.R., Dower, S.K., and Sims, J.E. (1996). Cloning of a putative ligand for the T1/ST2 receptor. J. Biol. Chem. *271*, 5784–5789.

Griffiths, G. (1993). Cryo and replica techniques for immunolabeling. In: Fine Structure Immunocytochemistry, Berlin: Springer Verlag, 137–203.

Griffiths, G., Ericsson, M., Krijnse Locker, J., Nilsson, T., Goud, B., Söling, H.D., Tang, B.L., Wong, S.H., and Hong, W. (1994). Localization of the Lys, Asp, Glu, Leu tetrapeptide receptor to the Golgi complex and the intermediate compartment in mammalian cells. J. Cell Biol. *127*, 1557–1574.

Kawano, J., Ide, S., Oinuma, T., and Suganuma, T. (1994). A protein-specific monoclonal antibody to rat liver β 1→4 galactosyltransferase and its application to immunohistochemistry. J. Histochem. Cytochem. *42*, 363–369.

Keown, W.A., Campbell, C.R., and Kucherlapati, R.S. (1990). Methods for introducing DNA into mammalian cells. Methods Enzymol. *185*, 527–537.

Kreis, T.E. (1986). Microinjected antibodies against the cytoplasmic domain of vesicular stomatitis virus glycoprotein block its transport to the cell surface. EMBO J. *5*, 931–941.

Marzioch, M., Henthorn, D.C., Herrmann, J.M., Wilson, R., Thomas, D.Y., Bergeron, J.J.M., Solari, R.C.E., and Rowley, A. (1999). Erp1p and Erp2p, partners for Emp24p and Erv25p in a yeast p24 complex. Mol. Biol. Cell *10*, 1923–1938.

Nakamura, N., Yamazaki, S., Sato, K., Nakano, A., Sakaguchi, M., and Mihara, K. (1998). Identification of potential regulatory elements for the transport of emp24p. Mol. Biol. Cell *9*, 3493–3503.

Nilsson, T., Pypaert, M., Hoe, M.H., Slusarewicz, P., Berger, E.G., and Warren, G. (1993). Overlapping distribution of two glycosyltransferases in the Golgi apparatus of HeLa cells. J. Cell Biol. *120*, 5–13.

Palmer, D.J., Helms, J.B., Beckers, C.J., Orci, L., and Rothman, J.E. (1993). Binding of coatomer to Golgi membranes requires ADP-ribosylation factor. J. Biol. Chem. *268*, 12083–12089.

Presley, J.F., Cole, N.B., Schroer, T.A., Hirschberg, K., Zaal, K.J.M., and Lippincott-Schwartz, J. (1997). ER-to-Golgi transport visualized in living cells. Nature *389*, 81–85.

Rabouille, C., Hui, N., Hunte, F., Kieckbusch, R., Berger, E.G., Warren, G., and Nilsson, T. (1995). Mapping the distribution of Golgi enzymes involved in the construction of complex oligosaccharides. J. Cell Sci. *108*, 1617–1627.

Rojo, M., Pepperkok, R., Emery, G., Kellner, R., Stang, E., Parton, R.G., and Gruenberg, J. (1997). Involvement of the transmembrane protein p23 in biosynthetic protein transport. J. Cell Biol. *139*, 1119–1135.

Roth, J., and Berger, E.G. (1982). Immunocytochemical localization of galactosyltransferase in HeLa cells: codistribution with thiamine pyrophosphatase in the trans-Golgi cisternae. J. Cell Biol. *93*, 223–229.

Rothman, J.E. (1994). Mechanisms of intracellular protein transport. Nature *372*, 55–63.

Rowe, T., and Balch, W.E. (1995). Expression and purification of mammalian Sar1. Methods Enzymol. *257*, 49–53.

Saraste, J., and Kuismanen, E. (1984). Pre- and post-Golgi vacuoles operate in the transport of Semliki Forest virus membrane glycoproteins to the cell surface. Cell *38*, 535–549.

Saraste, J., and Svensson, K. (1991). Distribution of the intermediate elements operating in ER to Golgi transport. J. Cell Sci. *100*, 415–430.

Scales, S.J., Pepperkok, R., and Kreis, T.E. (1997). Visualization of ER-to-Golgi transport in living reveals a sequential mode of action for COPII and COPI. Cell *90*, 1137–1148.

Schimmöller, F., Singer-Krüger, B., Schröder, S., Kruger, U., Barlowe, C., and Riezman, H. (1995). The absence of Emp24p, a component of ER-derived COPII-coated vesicles, causes a defect in transport of selected proteins to the Golgi. EMBO J. *14*, 1329–1339.

Shima, D.T., Cabrera-Poch, N., Pepperkok, R., and Warren, G. (1998). An ordered inheritance strategy for the Golgi apparatus: visualization of mitotic disassembly reveals a role for the mitotic spindle. J. Cell Biol. *141*, 955–966.

Sohn, K., Orci, L., Ravazzola, M., Amherdt, M., Bremser, M., Lottspeich, F., Fiedler, K., Helms, J.B., and Wieland, F.T. (1996). A major transmembrane protein of Golgi-derived COPI-coated vesicles involved in coatomer binding. J. Cell Biol. *135*, 1239–1248.

Stamnes, M.A., Craighead, M.W., Hoe, M.H., Lampen, N., Geromanos, S., Tempst, P., and Rothman, J.E. (1995). An integral membrane component of coatomer-coated transport vesicles defines a family of proteins involved in budding. Proc. Natl. Acad. Sci. USA *92*, 8011–8015.

Storrie, B., White, J., Röttger, S., Steltzer, E.H.K., Suganuma, T., and Nilsson, T. (1998). Recycling of Golgi resident glycosyltransferases through the ER reveals a novel pathway and provides an explanation for nocodazole induced Golgi scattering. J. Cell Biol. *143*, 1505–1521.

Tang, B.L., Peter, F., Krijnse-Locker, J., Low, S.H., Griffiths, G., and Hong, W. (1997). The mammalian homolog of yeast Sec13p is enriched in the intermediate compartment and is essential for protein transport from the endoplasmic reticulum to the Golgi apparatus. Mol. Cell. Biol. *17*, 256–266.

Wada, I., Rindress, D., Cameron, P.H., Ou, W.J., Doherty, J.J.D., Louvard, D., Bell, A.W., Dignard, D., Thomas, D.Y., and Bergeron, J.J. (1991). SSR α and associated calnexin are major calcium binding proteins of the endoplasmic reticulum membrane. J. Biol. Chem. *266*, 19599–19610.

Watzele, G., Bachofner, R., and Berger, E.G. (1991). Immunocytochemical localization of the Golgi apparatus using protein-specific antibodies to galactosyltransferase. Eur. J. Cell Biol. *56*, 451–458.

Yang, W., and Storrie, B. (1998). Scattered Golgi elements during microtubule disruption are initially enriched in *trans*-Golgi proteins. Mol. Biol. Cell *9*, 191–207.